CHEMISTRY OF MATERIALS
Cite This: Chem. Mater. 2017, 29, 9536-9546
Article
pubs.acs.org/cm

Designed Peptoids as Tunable Modifiers of Zeolite Crystallization

Rui Li,[†] Alisa Smolyakova,[‡] Galia Maayan,*[,‡] and Jeffrey D. Rimer*[,†]

[†]Department of Chemical and Biomolecular Engineering, University of Houston, Houston, Texas 77096, United States
[‡]Schulich Faculty of Chemistry, Technion-Israel Institute of Technology, Technion City, Hailfa 32000, Israel

Supporting Information

ABSTRACT: Peptides are among the most efficient classes of crystal growth modifiers for a wide range of natural and synthetic systems owing to their unmatched design space that affords the opportunity to construct highly specific sequences to tailor crystal growth. In the case of zeolite crystallization, the high pH and temperature of common synthesis conditions renders peptides ineffective for such applications. Here, we introduce peptoids as a biomimetic platform for the rational design of zeolite growth modifiers. The chemical robustness of peptoids coupled with their facile and efficient synthesis on solid support, which enables the generation of versatile sequences with diverse chemical functionality, make these materials ideal for the relatively harsh conditions of zeolite crystallization. A library of peptoids incorporating combinations of alcohol, amine, ether, and aromatic functional moieties were synthesized and tested in growth solutions of zeolite L (LTL type), a common commercial material. Our findings reveal that peptoids are potent modifiers of zeolite L crystallization. Syntheses with 1 wt % are often sufficient to suppress nucleation, indicating a strong interaction between peptoids and the amorphous precursors formed during the early stages of zeolite L synthesis. Chemical analysis reveals that a significant fraction of peptoid remains intact at pH 13 and 160 °C, though peptoid degradation occurs with prolonged hydrothermal treatment. Time-resolved analysis of products removed from zeolite L growth mixtures reveals that amines interact more favorably than alcohols with precursors/crystals. Our studies also confirm that peptoids can be tailored to either increase or decrease the length-to-width aspect ratio of cylindrical zeolite L crystals through the insertion of hydrophilic or hydrophobic groups, respectively. The mechanisms of peptoid action are discussed within the context of complex nonclassical pathways of zeolite crystallization. Moreover, this study provides the first testing and validation of peptoids as zeolite growth modifiers, thus opening new avenues in the future to extend this general platform to other zeolite framework types and related materials grown under conditions that are too severe for biomolecules.

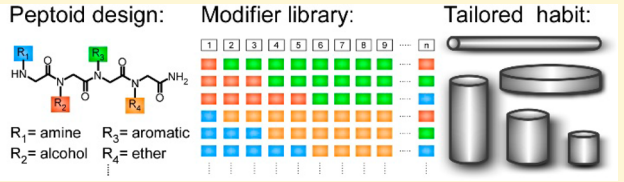

INTRODUCTION

Zeolites are microporous aluminosilicates with diverse applications that span traditional energy[1,2] and manufacturing areas to less traditional areas such as sensor technologies[3] and medicine.[4] A pervasive challenge in zeolite science is the control of crystallization to tailor their physicochemical properties. Zeolites grow by a combination of classical (*i.e.*, monomer-by-monomer addition) and nonclassical pathways[5] involving complex precursors that include oligomeric species, nanoparticles,[6] and bulk amorphous phases.[7] Establishing platforms for materials design without *a priori* knowledge of growth mechanisms and related methods to tune the multitude of synthesis conditions afforded to zeolites is nontrivial. One facile strategy for the rational design of crystalline materials is the employment of additives referred to as crystal growth modifiers (or alternatively auxiliaries, imposters, or inhibitors). This methodology is utilized in biomineralization,[8−11] living organisms,[12,13] and synthetic crystallization processes.[14,15] In brief, modifiers control the anisotropic growth rates of crystals by selectively binding to crystal surfaces and hindering the attachment of growth units.[8,16] The driving force(s) for modifier binding to crystal surfaces can involve a variety of interactions that include (but are not limited to) electrostatics,[8] epitaxial relations,[17] matching water affinity,[18] and hydrophobicity.[19,20] Prior studies have revealed that small variations in modifier structure and/or functionality can lead to dramatic changes in their specificity or efficacy.[19,21]

In cases where crystals grow classically through layer-by-layer mechanisms, modifiers tend to operate by attaching to specific surface sites (*e.g.*, kinks, step edges, or terraces)[9,10] and inhibit growth *via* kink blocking[22,23] or step pinning[24] modes of action to reduce the rate of step advancement on crystal surfaces.[9,10,16] For materials that grow by nonclassical pathways, such as zeolites, the role of modifiers can be convoluted by the presence of multiple precursors.[5,25] Modifiers may alter the formation and evolution of precursors,[26,27] and/or act by a classical mode of binding to crystal surfaces and impeding growth unit attachment. Examples of modifiers used in zeolite synthesis include small organics,[12,19] surfactants,[27−29] and polymers.[19,27] Macromolecules tend to be effective modifiers owing to their proximal binding moieties that can simultaneously bind to crystal surfaces. In literature, some of the most effective growth modifiers identified in biological and synthetic crystallization are macromolecules such as polymers,[30,31]

Received: September 7, 2017
Revised: October 11, 2017
Published: October 13, 2017

DOI: 10.1021/acs.chemmater.7b03798
Chem. Mater. 2017, 29, 9536−9546

DNA,[32] proteins,[20,33,34] and peptides.[8,35,36] An advantage of macromolecular modifiers is their relatively high potency (*i.e.*, effectiveness at low concentration).[19] The commercial viability of zeolite growth modifiers is related to inexpensive organics and the potential to recover modifiers postsynthesis for recycling. The harsh conditions of zeolite syntheses, such as high pH (11−14) and temperature (100−180 °C), make it impossible to employ peptides or other biomolecules. Peptides can degrade at even moderate thermal and chemical conditions.[37] To this end, materials with chemical robustness for these conditions must be found as alternatives.

One example of a biomimetic macromolecule with excellent thermal/chemical stability and highly designable sequences that can be prepared by simple solid-phase synthesis is (poly)-peptoids.[38] As shown in Scheme 1, peptoids are N-substituted

Scheme 1. General Structures of (A) Peptides and (B) Peptoids

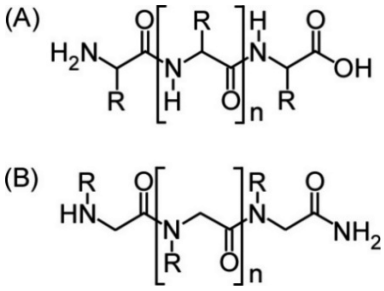

glycines with the side chains appended to the nitrogen rather than the α-carbon in peptides.[39] The removal of a stereogenic center and hydrogen bond donor (*i.e.*, hydrogen that is connected to N) renders peptoids achiral and lacking hydrogen bonds,[40,41] thus acquiring resistance to most conditions that would readily degrade peptides.[42] Prior studies have found that peptoids can form α-helices similar to peptides but are less affected by environmental conditions such as concentration, ionic strength, and solvent selection. They possess extraordinary thermal stability[42] and proteolytic degradation resistance.[43,44] The tertiary nitrogen in the peptoid backbone does not form hydrogen bonds, which allows for greater flexibility and chain rearrangement,[45,46] while achirality enables the formation of flat sheets with nanometer thickness and high aspect ratio.[39,46] Moreover, peptoid synthesis by a submonomer solid-phase synthesis strategy[38] enables interchangeable side chains,[47] thus permitting the rational design of sequences[48] with properties that are similar to peptides.[41,49,50]

Interestingly, the use of peptoids as crystal growth modifiers is less explored.[51] Many of the reported examples focus on tailoring the growth of biominerals[21,52] and mediating the aggregation of metal nanoparticles,[53−55] with a few studies reporting on ice[56] and gas hydrates.[57] Amphiphilic peptoids have been used to control calcite crystal morphology and accelerate its rate of growth under specific conditions.[52] The fact that peptoids can serve as both a particle stabilizer[54] and particle aggregation promoter[53] seems to suggest they can be designed with multiple functionality. Here, we capitalize on the unique properties of peptoids to design and test them as modifiers of zeolite L (LTL type). As shown in Figure 1, zeolite L crystals have a Si/Al ratio of 3 and a cylindrical habit. Their one-dimensional channels align axially in the [001] direction with diameters of *ca.* 7.1 Å, which is ideal for hosting organic

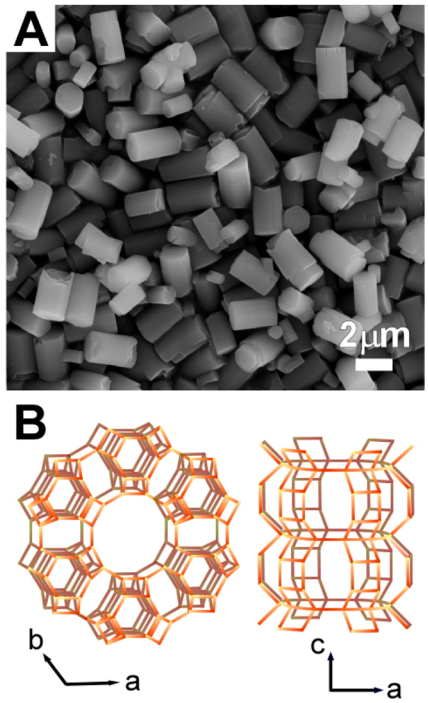

Figure 1. (A) Scanning electron micrograph of LTL crystals with cylindrical morphology. (B) Crystal structure of zeolite L (LTL) with one-dimensional channels (0.7 nm diameter) that are aligned axially along the [001] direction.

molecules in photonic devices (*i.e.*, dye incorporation)[3] and drug delivery scaffolds.[4]

The high thermal stability and shape selectivity of zeolite L is also utilized in catalytic reactions to produce value-added chemicals, such as aromatics[2] (*e.g.*, the commercial Chevron Aromax cyclization process[58]). There have been many studies aimed at optimizing the size and morphology of zeolite L crystals. The more successful approaches include the adjustment of synthesis parameters, such as water content, alkalinity, and temperature.[2,59−62] Compared to these strategies, a unique advantage of using modifiers is that they can be added to a zeolite growth solution in small quantity (≤1 wt %) without altering other synthesis conditions.

Herein, we explore zeolite L growth modification using a library of 16 peptoids with a range of binding moieties (alcohols and amines) as well as hydrophilic (ethers) and hydrophobic (aromatic) groups. Our findings provide the first confirmation that peptoids can be used as zeolite growth modifiers. Many of the peptoids selected for this study strongly inhibit the kinetics of zeolite L crystallization. At sufficiently high concentration (*ca.* 1 wt %), we demonstrate that peptoids are capable of suppressing nucleation. Comparison of hydrophilic and hydrophobic peptoids reveal the ability to alter zeolite L crystal morphology, while our findings indicate that hydrophobicity may not play a dominant role as previously proposed. We also discuss the nonclassical pathways of zeolite crystallization, offer new perspectives on zeolite growth modifiers, and posit the role(s) of peptoids as inhibitors of zeolite L nucleation and crystal growth.

EXPERIMENTAL SECTION

Materials. The following chemicals for zeolite synthesis were purchased from Sigma-Aldrich (St. Louis, MO, USA): LUDOX AS-40 (40 wt % suspension in water), potassium hydroxide (85% pellets),

DOI: 10.1021/acs.chemmater.7b03798
Chem. Mater. 2017, 29, 9536−9546

and aluminum sulfate hydrate (98%, calculated as 1:18 $AlSO_4$:H_2O). The following chemicals for peptoids synthesis were purchased from various suppliers: Rink Amide resin (Novabiochem), trifluoroacetic acid (TFA, Alfa Aesar), bromoacetic acid (MERCK), *N*,*N*′-diisopropylcarbodiimide (DIC, Sigma-Aldrich), piperidine (Sigma-Aldrich), acetonitrile (CAN, Sigma-Aldrich), water HPLC grade solvents (Sigma-Aldrich), dimethylforamide (DMF, Bio-Lab Ltd.), and dichloromethane (DCM, Bio-Lab). Deionized (DI) water used in all experiments was purified with an Aqua Solutions RODI-C-12A purification system (18.2 MΩ). All reagents and solvents were used as received without further purification, with the exception of DMF that was dried with molecular sieves.

Peptoid Synthesis. Peptoids were synthesized either on solid phase (resin) using the standard procedure, which follows the submonomer approach, or in solution. For the on resin method, peptoids were synthesized manually on Rink Amide resin at room temperature using the submonomer approach. Typically, 100 mg of resin was swollen in DCM for 40 min before initiating oligomer synthesis. Multiple washing steps using DMF were performed between each step described below. Fmoc deprotection of resin was performed by the addition of 20% piperidine solution (2 mL in DMF), and the reaction was allowed to shake at room temperature for 20 min. Following the reaction, piperidine was washed from the resin using DMF (1 mL × 3 × 1 min). Bromoacetylation was completed by adding bromoacetic acid (1.2 M in DMF, 850 μL) and DIC (200 μL); this reaction was allowed to shake at room temperature for 20 min. Following the reaction, the bromoacetylation reagents were washed from the resin using DMF and primary amine (1.0 M in DMF) was added. The amine displacement reaction was allowed to shake at room temperature for 20 min and was followed by multiple DMF washing steps. Bromoacetylation and amine displacement steps were repeated until the required peptoids were obtained. To cleave the peptoid oligomers from solid support for analysis, approximately 5 mg of resin was treated with 95% TFA in water (1 mL) for 10 min. The cleavage cocktail was evaporated under nitrogen gas and the peptoid oligomers were resuspended in 500 μL of HPLC solvent (1:1 ACN:H_2O HPLC grade). To cleave the peptoid oligomers from solid support for preparative HPLC, the beads were treated with 5 mL of 95% TFA in water for 30 min. The cleavage cocktail was evaporated under low pressure, resuspended in 2 mL HPLC solvents mixture, and lyophilized overnight.

Using the solution-phase method, peptoid dimers were synthesized in an iterative fashion under N_2 stream according to Supporting Information Figure S1. In the first step, bromoacetamide was generated from reaction of dimethyl amine chloride with bromoacetyl bromide at −78 °C by using dichloromethane as the solvent.[63] Nucleophilic substitutions and following bromoacetylations were performed at 0 °C using tetrahydrofuran as the solvent.[64] These synthetic steps proceed with relatively high efficiency to give crude products. For deprotection of functional groups, the crude products were treated with TFA at 0 °C and the pure peptoid was isolated by preparative HPLC.

Peptoid Stability Test. The stability of a representative peptoid, Nae−$(Nme)_6$, was tested under the harsh conditions of zeolite synthesis (*i.e.*, high solution alkalinity and elevated synthesis temperature). For simplicity, both silica and aluminum were omitted from the solution. Around 40 mg peptoid was added into 4 g of 1 M KOH solution (pH 13.91) to maintain the same peptoid concentration (1 wt %) as that of the zeolite synthesis solution. The peptoid-containing high-pH solution was hydrothermally treated under the same zeolite synthesis conditions at about 160 °C, cooled, neutralized with HCl, and then dried for compositional analysis.

Zeolite Crystallization and Characterization. Zeolite L crystals were synthesized using K^+ as an inorganic structure-directing agent. Growth solutions were prepared using a reported protocol[7,65] with a molar composition of 0.51:20:10.2:1030 Al_2O_3:SiO_2:K_2O:H_2O. In a typical experiment, potassium hydroxide (0.25 g) was dissolved in DI water (3.11 g), followed by the addition of aluminum sulfate (0.066 g). This solution was stirred until it became clear (*ca.* 5 min). LUDOX AS-40 (0.57 g) was then added, and the resulting solution was left to stir overnight (*ca.* 21 h) at room temperature (referred to as the aging period). Peptoids were added 2 h prior to the completion of aging with a concentration of 1 wt % peptoid, unless otherwise noted. After aging was complete, the growth solution (*ca.* 4 g) was placed in a Teflon-lined stainless steel acid digestion bomb (Parr Instruments) and was heated under static conditions (*i.e.*, without mixing) in a ThermoFisher Precision Premium 3050 Series gravity oven at 160 °C and autogenous pressure for 5 days. The zeolite L growth solution and resulting crystals prepared without peptoid are referred to herein as the *control*. For X-ray and microscopy analyses, the particulates in the growth solution (amorphous and/or crystalline) were isolated as a white powder by centrifugation (Beckman Coulter Avanti J-E series high-speed centrifuge) at 13,000 rpm for 45 min. The solid was washed with DI water to remove the supernatant, and the centrifuge/washing cycle was repeated a second time. The resulting gel was dried at ambient conditions. Samples for electron microscopy were prepared by placing an aliquot of supernatant on a glass slide and drying in air. Crystals on the glass slide were transferred to sample holders (Ted Pella) by gently pressing the glass slide on carbon tape.

Instrumentation. Peptoid oligomers analysis was done by RP-HPLC using a Jasco UV-2075 PLUS detector on a Phenomenex Luna C-18 column (5 μm, 100 Å, 2.0 × 50 mm^2, a linear gradient of 5−95% ACN in water (0.1% TFA) over 10 min was used at a flow rate of 700 μL/min) or Primesep 200 (5 μm, 100 Å, 2.1 × 150 mm^2, a linear gradient of 5−95% ACN in water (0.1% TFA) over 10 min was used at a flow rate of 200 μL/min). Purification of peptoid oligomers was performed by preparative HPLC using a Jasco UV-2075 PLUS detector on a Phenomenex AXIA Packed Luna C-18 column (15 μm, 100 Å, 21.20 × 100 mm^2). Peaks were eluted with a linear gradient of 5−95% ACN in water (0.1% TFA) over 50 min at a flow rate of 5 mL/min. Peptoid oligomers were identified by mass spectrometry analysis done on an Advion expression CMS mass spectrometer under electrospray ionization (ESI) using a direct probe, with samples running in 95% aqueous acetonitrile (0.1% formic acid) at a flow rate of 0.2 mL/min. Solids extracted from zeolite L growth solutions were characterized by powder X-ray diffraction (XRD) using a Siemens D5000 X-ray diffractometer with Cu Kα radiation (40 kV, 30 mA, 1.54 Å). Scanning electron microscopy (SEM) was performed with a FEI 235 dual-beam (focused ion beam) system operated at 15 kV and a 5 mm working distance. All SEM samples were coated with a thin layer of carbon (*ca.* 30 nm) prior to imaging.

RESULTS AND DISCUSSION

Peptoid Synthesis and Hydrothermal Stability. Previous studies have shown that molecules or macromolecules decorated with hydroxyl[19] or amine[27] groups tend to be effective zeolite growth modifiers (ZGMs), resulting in moderate to substantial changes in crystal morphology.[12,19,26,27] In order to construct a library of peptoids as designable ZGMs, we synthesized 16 different sequences (Figure 2) of varying size derived from combinations of five building units with varying functional R groups: alcohol (Nhe), amine (Nae), ether (Nme), benzene (Npm), and methyl (dma). The majority of peptoids are terminated with a primary amine, but in certain cases a tertiary amine is used (*i.e.*, -$N(CH_3)_2$, dma). Peptoid sequences are listed with subscripts (*m* or *n*) denoting the number of sequential building units.

A common concern when using organics in zeolite synthesis, be it a modifier or structure-directing agent, is whether the harsh conditions will lead to degradation. Alkaline solutions (pH 12−14) and high temperatures (>100 °C) used for zeolite synthesis can induce chemical modifications in organics, potentially sacrificing their efficacy as modifiers. Zeolite L is prepared at pH 13 and 160 °C, making it one of the more severe conditions among zeolites to test the stability of peptoids. In order to assess peptoid stability, we selected

DOI: 10.1021/acs.chemmater.7b03798
Chem. Mater. 2017, 29, 9536−9546

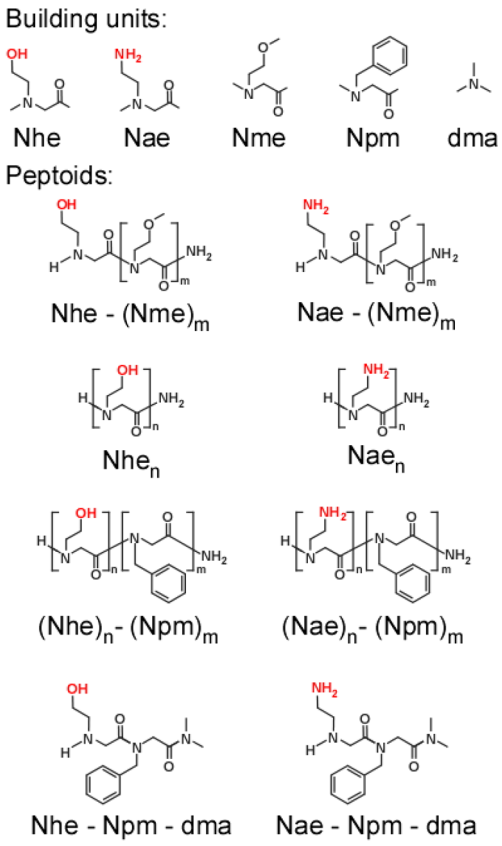

Figure 2. Peptoid building units and the corresponding library of modifiers synthesized for this study. The nomenclature of each peptoid is provided where blocks of a particular building unit are denoted with subscripts *m* or *n*, which indicate the total number of each building unit in the primary sequence. Common ZGM moieties (*i.e.*, alcohol and amine groups) are highlighted in red.

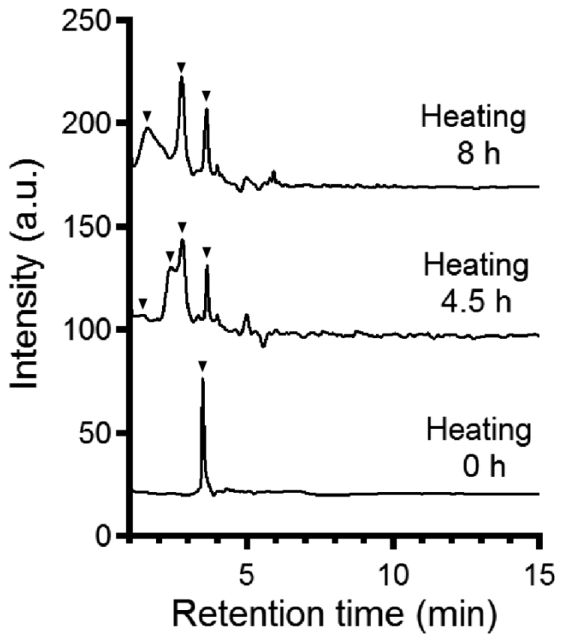

Figure 3. Time-elapsed HPLC patterns demonstrating the partial degradation of peptoid molecules. Patterns of the original peptoid Nae−$(Nme)_6$ (0 h) are compared to those after hydrothermal treatment at the same condition of zeolite L synthesis for 4.5 and 8 h. The emergence of peaks at lower retention times while the original peak position for Nae−$(Nme)_6$ is maintained (at least up to 8 h of heating) indicate partial degradation. For a sample after 1 day of hydrothermal treatment (not shown), the complete absence of peaks indicates the full degradation of peptoid.

Nae−$(Nme)_6$ and first analyzed the as-made peptoid by HPLC (Figure 3, 0 h) to confirm its purity.

The peptoid was hydrothermally treated in a pseudozeolite mixture of KOH solution (pH 14) that was heated at 160 °C for periodic times. The HPLC patterns of peptoids after heat treatment for 4.5 and 8 h are shown in Figure 3. These times roughly correspond to the assembly of amorphous precursors and the induction period, respectively.[7] The peak attributed to Nae−$(Nme)_6$ (retention time = 3.6 min) is present throughout hydrothermal treatment, though its loss of intensity is consistent with the progressive appearance of peaks at lower retention times, indicating a partial degradation of the peptoid heptamer. Mass spectroscopy analysis of peaks at 2.8 and 2.4 min retention times reveals that they correspond to tetramers and tetramer fractions with both the removal of a functional group and two monomers, whereas the broad peak at 1.9 min retention time appears to be smaller species including a small fraction of the tetramers (see Figure S2). Provided that the peptoid is introduced in zeolite growth solutions at a concentration that maintains the desired level of nondegraded modifier, the peptoid is stable for sufficient time to influence zeolite nucleation (*ca.* 8 h) and crystal growth, which requires an additional *ca.* 14 h of heating time.[7] Segmented fractions of the peptoid that degrade with time could also act as additional modifier(s). It should be noted that the conditions for zeolite L synthesis are significantly more severe than those of many other zeolite framework types (*e.g.*, FAU, LTA, GIS, SOD, and EMT, *etc.*).[66,67] Notably, the latter require lower temperatures (≤100 °C), which would extend modifier lifetime and dramatically reduce the degree of peptoid degradation.

Peptoid Modification of Zeolite L Morphology. Prior studies have demonstrated that surfactants can have a pronounced impact on zeolite crystallization.[28,29] Here, we emulated this class of modifiers by synthesizing an amphoteric peptoid comprised of hydrophobic benzene residues (Npm) and a hydrophilic alcohol residue (Nhe) to mimic surfactant tail and head groups, respectively. In this study the same zeolite growth solution was divided into two batches, one containing the peptoid and one without any additive (referred to as the control). As shown in Figure 4A, the peptoid Nhe−$(Npm)_6$ reduces the [001] length of zeolite L crystals from a nominal value of 1.5 ± 0.2 to 1.0 ± 0.2 μm in the presence of 1 wt % peptoid. A similar measurement was performed with another peptoid wherein the hydrophobicity of the tail was reduced by switching from benzene to a methyl ether residue (Nme). If we consider the octane−water partition coefficient, f_{oct}, which is an indicator of hydrophobicity, a switch from benzene to ether leads to a substantial change in peptoid hydrophobicity: $f_{benzene}$ = 1.90 and $f_{-CH_2-O-CH_3}$ = −0.30. As shown in Figure 4B, this reduction in hydrophobicity has the opposite effect on crystal habit. The control sample for the second batch had a slightly broader distribution (length = 1.4 ± 0.4 μm); and in the presence of Nhe−$(Nme)_6$, we observe an increase in the [001] length of zeolite L crystals to 1.9 ± 0.5 μm. This effect was achieved using a small quantity of modifier (*i.e.*, 0.5 wt % peptoid), which is characteristic of most macromolecules (*e.g.*, polymers).[19] Thermogravimetric analysis of the control and peptoid-modified crystals reveals comparable weight loss

DOI: 10.1021/acs.chemmater.7b03798
Chem. Mater. 2017, 29, 9536−9546

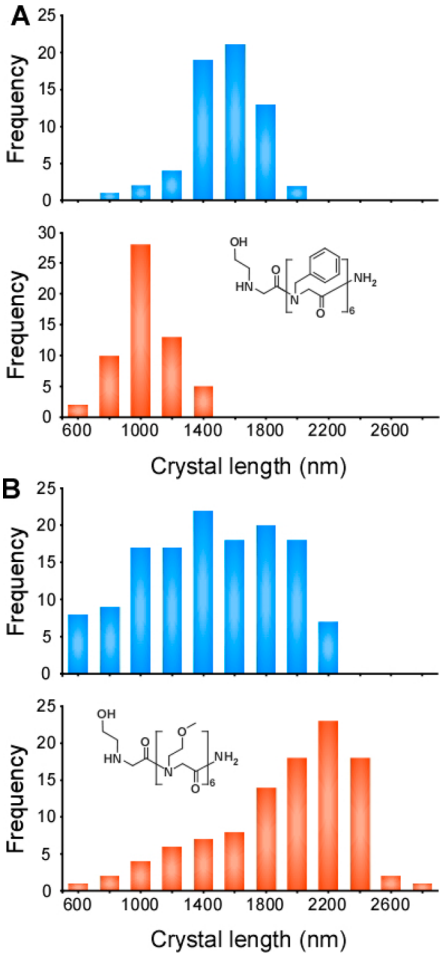

Figure 4. Comparison of zeolite L crystal dimensions along the [001] direction. (A) Synthesis in the absence of modifier (top, blue) and in the presence of 1 wt % Nhe−$(Npm)_6$ (bottom, orange) reveals a reduction in length in the presence of the peptoid. (B) A separate synthesis batch in the absence of modifier (top, blue) and in the presence of 0.5 wt % Nhe−$(Nme)_6$ (bottom, orange) reveals a net increase in length. Data for each batch were collected from 100 crystals in scanning electron micrographs.

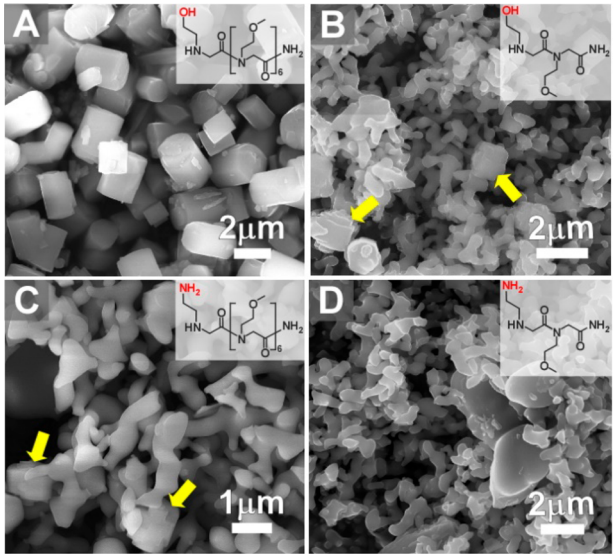

Figure 5. Effects of short- and long-chain peptoids on zeolite L crystallization. Scanning electron micrographs depict representative images of the products from growth solutions prepared with the following peptoids: (A) Nhe−$(Nme)_6$, (B) Nhe−Nme, (C) Nae−$(Nme)_6$, and (D) Nae−Nme. Solids were extracted from growth solutions containing 1 wt % peptoid after heating at 160 °C for 5 days. Corresponding powder XRD patterns are provided in Figure 6. Particles in image A are purely crystalline whereas those in image D are predominantly amorphous. Images B and C depict partially crystalline products where the yellow arrows indicate cylindrical particles resembling LTL crystals.

(Figure S3), indicating that the modifier is not retained within the pores of the zeolite, thus allowing for the potential recovery of peptoids. Moreover, measurements of solution pH show that the addition of peptoids does not alter the alkalinity of the growth medium.

Peptoid Impact on the Kinetics of Crystallization. Here we investigate two distinct properties of peptoids synthesized for this study: (1) the length of the primary sequence (*i.e.*, number of monomers) and (2) the selection of hydrophobic terminal groups. Focusing on ether-containing (Nme) peptoids, we selected two building units as terminal groups comprised of either alcohol (Nhe) or primary amine (Nae) functional moieties. Comparison of crystals prepared in the presence of peptoids with an alcohol terminal group (Nhe−$(Nme)_6$, Figure 5A) to that of an amine-containing group (Nae−$(Nme)_6$, Figure 5C) reveals that the latter more effectively inhibits crystallization. This is confirmed by powder X-ray diffraction (XRD) patterns of the samples that reveal marked differences in the amounts of residual amorphous precursor. Indeed, subtle differences in peptoid structure (*i.e.*, the interchange of a single monomer) reveals that the amine is a more potent modifier, which is qualitatively consistent with our previous finding that propylamine (or butylamine) is a more effective ZGM than propanol (or butanol);[19] however, differences between alcohol and amine groups on peptoids are more pronounced. Moreover, we unexpectedly observed that a reduction in the size of the peptoid results in more potent inhibitors of crystal growth. This is counter to most examples in crystal growth modification where the polymer tends to be significantly more effective than its corresponding monomer.[68] For instance, a reduction in the size of Nhe−$(Nme)_6$ to Nhe−Nme (Figure 5B) increased the percentage of amorphous material in the product. In the case of Nae−$(Nme)_6$, a reduction in its size to Nae−Nme (Figure 5D) resulted in complete suppression of crystallization. All four peptoids in Figure 5 are compared with the same mass (1 wt %) such that the total number of monomers is approximately the same.

In some instances we find that hydrophobicity can differentiate ZGM efficacy,[19] whereas in other cases it appears to be less critical. For example, the octanol−water partition coefficients[69] for amine and alcohol groups are comparable, $f_{NH_2} = -1.34$ and $f_{OH} = -1.45$, and likely do not account for the differences observed in Figure 5. One possible explanation could be differences in the degree of solvation for amines and alcohols, while another could be related to the charge bore by these moieties. For instance, in the highly alkaline zeolite L growth solution (pH = 14) the amines are expected to be neutral (*i.e.*, carrying no charge); however, the coexistence of positively charged amine species cannot be entirely ruled out.[70] On the contrary, alcohols are weakly acidic under such conditions and may carry a negative charge at high temperature.[71,72] Given that the surfaces of zeolites and amorphous

DOI: 10.1021/acs.chemmater.7b03798
Chem. Mater. 2017, 29, 9536−9546

precursors are negatively charged, it is reasonable to expect amines to more favorably interact with these interfaces.

Probing Steric Constraints on Peptoid−Crystal Interactions. It was mentioned that polymers tend to be more effective crystal modifiers compared to their respective monomers.[68] This is generally attributed to a macromolecule's ability to interact with multiple sites on crystal (or precursor) surfaces compared to smaller molecules that possess fewer binding moieties. Small molecules more rapidly desorb from surfaces, whereas the proximal binding groups of polymers can increase their residence time on substrates. Interestingly, the opposite trend seems to hold for the peptoids examined in this study. The reason for this phenomenon is not well understood, but one possible explanation could be the steric constraint(s) of bulky side chains that interfere with peptoid binding to the surfaces of zeolite crystals/precursors. To test this hypothesis, we examined peptoids with bulky rigid benzene groups (Npm).

Here we subdivide samples on the basis of peptoid N-terminal groups being either alcohols (Figure 6A) or amines

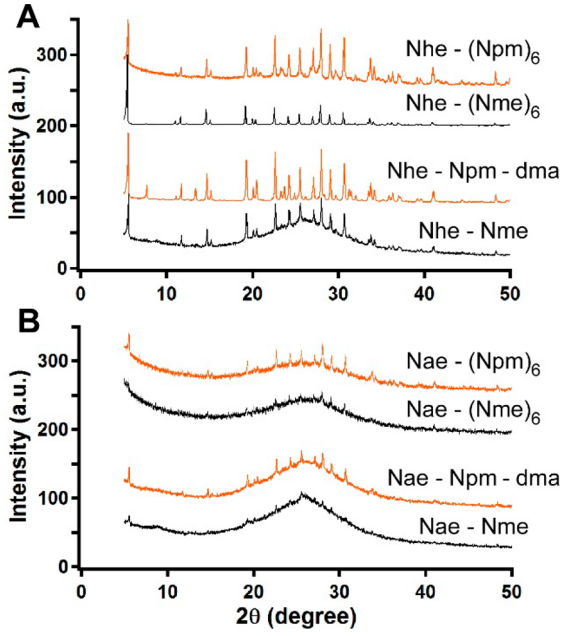

Figure 6. Powder X-ray diffraction patterns of solids extracted from zeolite L growth solutions after heating for 5 days at 160 °C in the presence of peptoids containing (A) alcohol (Nhe) and (B) primary amine (Nae) groups. Here we also assess the effect of adding a tertiary amine (dma) to the termini of peptoids Nhe−Npm and Nae−Npm to replace the primary amine in Npm.

(Figure 6B). Once again, amine-containing peptoids more effectively inhibit zeolite L crystallization. There is little difference between benzene- and ether-containing peptoids, suggesting that steric constraints are less critical. Powder XRD patterns of samples extracted after 5 days of heating reveal broad peaks in the range 2θ = 20−30° corresponding to the presence of residual amorphous material. We have shown that shorter peptoids as well as those with Nae (primary amine) groups increase the percentage of amorphous material in the final product owing to their ability to effectively inhibit zeolite nucleation. All peptoids also contain a primary amide at the C-terminus of their sequences, which seemingly has less impact on zeolite crystallization. To test this hypothesis, we modified the termini of peptoids Nhe−Npm and Nae−Npm (Figure S4) to contain tertiary amides (dma). This substitution had no appreciable effect on the products, which may indicate that functional groups in the primary backbone of peptoids are less critical in crystal growth inhibition than those decorating the side groups.

The difference between peptoids containing amine and alcohol moieties was examined more closely. We prepared peptoids with block copolymer-like motifs consisting of Npm paired with either Nae or Nhe. The total number of building units was fixed, while the ratio of hydrophobic segments (Npm) to hydrophilic segments (Nae or Nhe) was systematically varied. Scanning electron micrographs (Figure 7) and

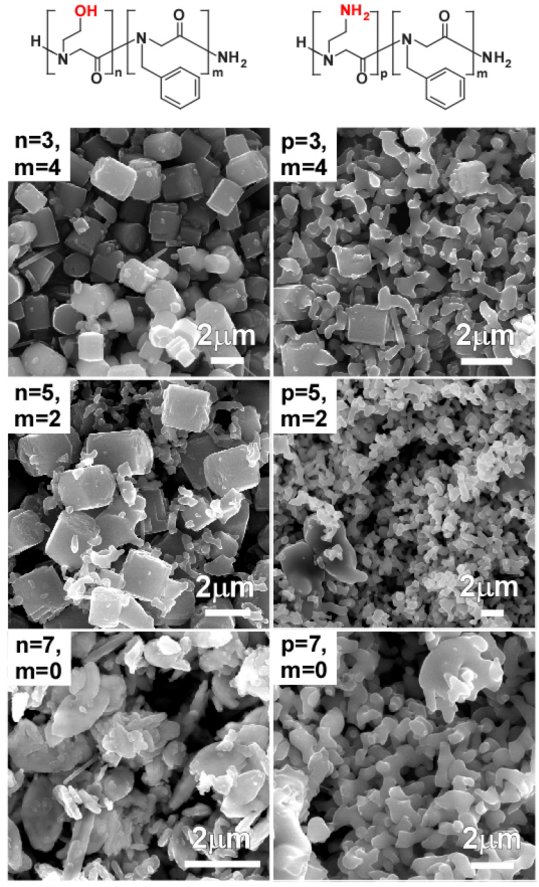

Figure 7. Sequential substitution of benzene groups (Npm, *m*) with the following moieties: (left column) alcohol groups (Nhe, *n*) and (right column) primary amine groups (Nae, *p*). The corresponding powder XRD patterns for these samples are provided in Figure 8.

powder XRD patterns (Figure 8) of the products extracted after 5 days heating at 160 °C reveal a progressive decrease in percent crystallinity as the number of benzene (Npm) groups are substituted with either alcohol (Nhe) or amine (Nae) groups. Peptoid Nhe_7, which is comprised of only alcohols, results in the crystallization of potassium hydrogen silicate ($KHSi_2O_5$). Peptoids comprised of ether residues (*e.g.*, Nae−$(Nme)_6$) lead to partially crystalline zeolite L whereas those comprised solely of primary amines (*e.g.*, Nae_7) yield an amorphous product. As will be discussed later, a shift from amorphous to crystalline product can be achieved using lower peptoid concentration. Based on these findings it appears that peptoids are more potent than polymeric modifiers previously identified for zeolite L crystallization, such as poly-

DOI: 10.1021/acs.chemmater.7b03798
Chem. Mater. 2017, 29, 9536−9546

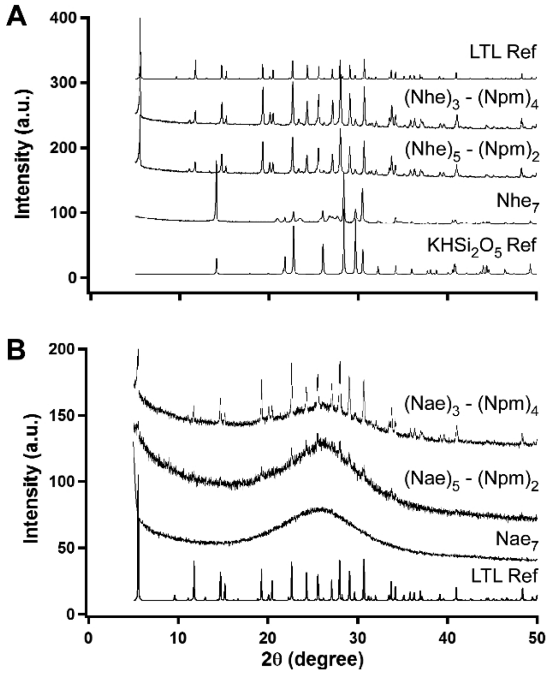

Figure 8. Powder XRD patterns for samples prepared with peptoid sequences (A) $(Nhe)_n(Npm)_m$ and (B) $(Nae)_p(Npm)_m$ with varying numbers of alcohol and primary amine groups, respectively. Reference patterns (labeled ref) for $KHSi_2O_5$ and zeolite L (LTL) are provided for comparison.

(diallyldimethylammonium chloride) (PDDAC) and 1-ethyl-1-methylpyrrolidinium bromide (EMPB).[19] Collectively, these findings indicate that peptoids should be used in lower concentration (≤0.5 wt %) to have the desired effect(s) on crystal growth while avoiding the formation of amorphous product.

Zeolites grow by a combination of classical and nonclassical mechanisms, which calls into question a modifier's mode of action. For instance, theories and experimental evidence of crystals that grow by classical layered mechanisms reveal that modifiers adsorb on crystal surfaces and impede solute attachment, thereby altering the rate(s) of anisotropic growth. The peptoids examined in this study as well as other ZGMs reported previously[12,19,26] may indeed act by similar mechanisms; however, nonclassical pathways lend additional complexity to identifying the exact mode of action for modifiers. Scheme 2 provides a general overview of the different pathways of zeolite L growth in the presence of amorphous precursors, highlighting putative growth units identified from time-resolved studies of zeolite L crystallization.[7] As previously reported,[73] colloidal silica used to prepare zeolite growth mixtures remains suspended in the alkaline solution throughout room temperature aging owing to the adsorption of alumina, which markedly reduces the rate of silica dissolution.[7] Upon heating, the colloidal particles agglomerate into small clusters (Scheme 2, steps ii and iii), often referred to as *worm-like particles* (WLPs).[7] WLPs grow *via* the addition of soluble species (Scheme 2, step i) until the end of the induction period when their size remains relatively constant while the population of precursors decreases with increased heating time (*i.e.*, WLPs are progressively consumed by zeolite L crystals).

There are two general pathways of zeolite L growth. The first involves the attachment of WLPs to crystal surfaces (Scheme 2, step iv). Evidence for this pathway is gleaned from SEM images

Scheme 2. Putative Pathways of Zeolite L Crystallization

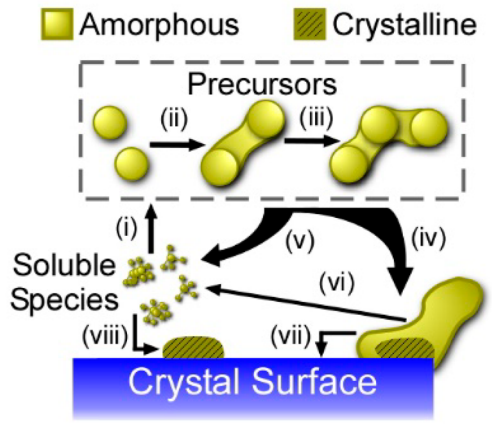

of solids extracted from growth solutions during an intermediate stage of hydrothermal treatment that show WLPs directly attached to crystal surfaces (*i.e.*, feeding nutrient directly to the growing interface).[7] In this scenario, amorphous WLPs undergo a disorder-to-order transition wherein the adsorbed WLP rearranges through solid (or gel) transformations at the crystal interface or *via* the release of (alumino)silicate species that reattach to the crystal surface (Scheme 2, step vii). A second pathway involves the attachment of soluble species (Scheme 2, step viii) where the supersaturation in the growth solution presumably can be maintained by WLP dissolution (Scheme 2, steps v and vi). The degree to which these multiple pathways contribute to zeolite L growth is not well understood; however, it is evident that peptoids have the potential to alter multiple steps.

The discussion until this point has been based on a working theory that modifiers function by adsorption to crystal surfaces;[8,52] however, recent evidence points to alternate routes for the inhibition of zeolite growth. For example, we have shown that the addition of polyamines to growth solutions of zeolite SSZ-13 (CHA) reduce precursor aggregation and evolution, leading to smaller crystals with sizes commensurate with those of a single precursor.[27] Modifiers in this scenario act as colloidal stabilizers rather than conventional adsorbates on crystal interfaces (although the latter cannot be precluded from the overall mechanism). In the same study, we observed that polymers with positively charged quaternary amines promote precursor attachment to SSZ-13 crystals and dramatically reduce the time of crystal growth. Collectively, these findings provide evidence that modifier−precursor interactions can influence zeolite crystallization.

An interesting observation in this study is the ability of peptoids to suppress zeolite L nucleation. It is less common in literature to find studies that are focused on modifier inhibition of nucleation. This phenomenon has not been previously observed for either small molecule or polymeric ZGMs. In Scheme 2 we omit details of zeolite L nucleation due to the lack of information on this topic. For other zeolite frameworks, such as FAU, EMT, and LTA, it is postulated that nucleation occurs on the exterior surfaces of amorphous precursors.[73−75] The same may be true for zeolite L, although there is no direct evidence to support this claim. If we hypothesize that WLPs provide sites for heterogeneous nucleation, then it is conceivable that peptoid−precursor interactions could suppress, or at least significantly delay, nucleation. It is not evident,

DOI: 10.1021/acs.chemmater.7b03798
Chem. Mater. 2017, 29, 9536−9546

however, how this scenario differs from polymer−precursor interactions in SSZ-13 synthesis where the induction time is either unaffected or reduced for neutral and positively charged ZGMs, respectively.

We have found that the presence of peptoids leads to an increase in the size of WLPs compared to the control (Figure 9). Typically, WLP growth/aggregation ceases around the end

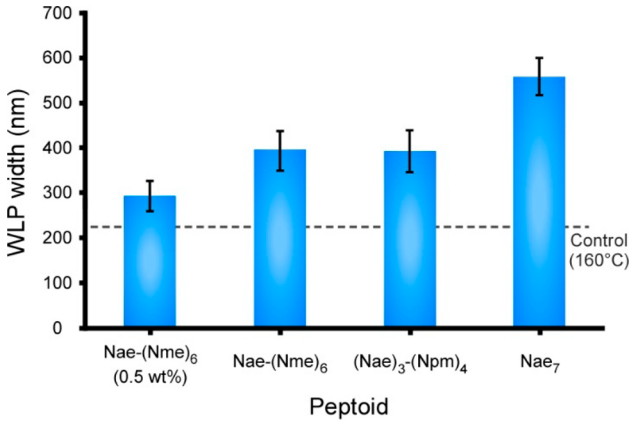

Figure 9. WLP size in zeolite L solutions containing peptoids of increasing efficacy (from left to right) as crystal growth inhibitors. All samples were synthesized at 160 °C for 5 days with the addition of 1 wt % peptoid (unless otherwise noted). In the control sample, WLPs reach a stable size at the end of the induction period, which is indicated by the dashed line (see Kumar *et al.*[7]). WLP sizes in the presence of peptoids are much larger, ranging from a 35 to 158% increase in size relative to the control. Data for each sample are the average of more than 70 WLPs analyzed in scanning electron micrographs. Error bars equal two standard deviations.

of the induction period (*i.e.*, when Bragg peaks are first detected in XRD patterns).[7] Many of the peptoids in Figure 1 either suppress or dramatically inhibit zeolite L nucleation, which would presumably allow WLPs to continue growing to larger sizes. This is observed in Figure 9 for peptoids with disparate efficacy (increasing from left to right). Interestingly, this observation is qualitatively consistent with previous findings that the induction time of zeolite L crystallization increases with increased WLP size; however, the exact role of peptoids in WLP formation/evolution and zeolite nucleation is not well understood.

Concentration Dependence of Peptoids. The majority of data presented to this point was gathered from syntheses using 1 wt % peptoid, which was sufficient in many cases to completely suppress zeolite L nucleation. Here, we examine the effect of reduced peptoid concentration, selecting two modifiers with different efficacy: Nae−$(Nme)_6$ and Nhe−$(Nme)_6$. The results for Nae−$(Nme)_6$ (Figure 10A−C) reveal a progressive increase in amorphous product with increasing peptoid weight percent. For instance, at 0.5 wt % electron micrographs (Figure 10B) contain residual WLPs that are consistent with the broad peak in powder XRD patterns at $2\theta = 20-30°$ (Figure 10C). In this case, 0.2 wt % would be an approximate upper limit for Nae−$(Nme)_6$. For less potent peptoids, such as Nhe−$(Nme)_6$, the modifier does not have a noticeable impact on zeolite nucleation. The concentration profile for Nhe−$(Nme)_6$ (Figure 10D) is similar to trends reported for other modifiers (*e.g.*, PDDAC, EMPB, and ethanol)[19] wherein there is a monotonic change in crystal size with increased modifier concentration, reaching a plateau at some threshold weight percentage, above

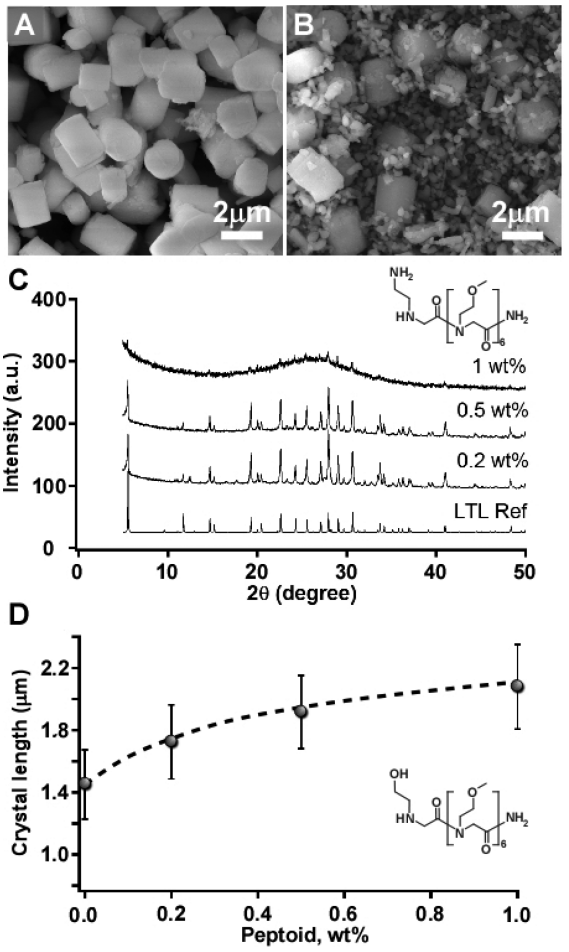

Figure 10. Effect of peptoid concentration on zeolite L crystallization. (A and B) Scanning electron micrographs of zeolite L modified by Nae−$(Nme)_6$ at the following concentrations: (A) 0.2 wt % and (B) 0.5 wt %. (C) Powder XRD patterns of Nae−$(Nme)_6$ samples at various weight percentages. A reference pattern for LTL (bottom) is provided for comparison. (D) [001] length of LTL crystals as a function of Nhe−$(Nme)_6$ weight percentage. Data are the average of more than 100 crystals. Error bars equal two standard deviations, and the dashed line is interpolated to guide the eye.

which an additional increase in modifier concentration does not lead to appreciable changes in crystal dimension. The plateau for Nhe−$(Nme)_6$ occurs around 1 wt %.

CONCLUSION

In summary, we have provided the first demonstration of peptoids as zeolite growth modifiers. The generation of a small library of peptoids with varying functional moieties and sizes allowed for the parametric evaluation of structure−performance relationships. Our findings indicate that peptoids are potent and require low concentrations (<1 wt %) to be effective modifiers of zeolite L crystallization. The functional motifs of these novel modifiers can be tailored to selectively increase or decrease the length-to-width aspect ratio of zeolite L crystals. Moreover, we show that ZGMs are capable of influencing early stages of nucleation, which suggests a strong interaction between peptoids and amorphous WLP precursors.

A distinct advantage of peptoids is their chemical and thermal stability, which makes them robust to the harsh conditions of zeolite synthesis. Prior studies have shown that

DOI: 10.1021/acs.chemmater.7b03798
Chem. Mater. 2017, 29, 9536−9546

peptoids can withstand high pH at moderate temperatures. In this study, we selected a set of conditions that fall within the extreme of zeolite synthesis to assess whether peptoids can withstand such circumstances. We observed a temporal degradation of peptoids to smaller segments with increased heating time; however, a significant fraction of the original peptoid remains intact throughout much of the nucleation and growth stages. To this end, careful attention should be paid to the relative time scales of zeolite crystallization and partial decomposition of peptoids, recognizing that the nature of the modifier could potentially change with time depending on the synthesis conditions. Given the fact that there are many zeolites synthesized in shorter time and/or at lower temperature than that of zeolite L, including many commercial frameworks, peptoids introduced as modifiers would be expected to remain intact for the duration of the synthesis.

The virtually unlimited design space for generating peptoids with tailored physicochemical properties offers a new approach for the rational design of zeolite growth modifiers. Future efforts to move this approach toward commercialization will require concerted efforts in peptoid synthesis (*i.e.*, economical scale up) and fundamental studies that elucidate their exact modes of action in zeolite crystallization. The latter is an ongoing area of research that is actively focused on developing predictive models to *a priori* identify modifiers for a range of zeolite framework types.

■ ASSOCIATED CONTENT

Supporting Information

The Supporting Information is available free of charge on the ACS Publications website at DOI: 10.1021/acs.chemmater.7b03798.

Details of materials characterization and analysis, including LCMS patterns for peptoid stability, TGA patterns indicating peptoid uptake in zeolite L, additional SEM images and XRD patterns of peptoid-modified zeolite L samples, and HPLC and LCMS patterns of all the peptoids synthesized (PDF)

■ AUTHOR INFORMATION

Corresponding Authors

*(J.D.R.) E-mail: jrimer@central.uh.edu.
*(G.M.) E-mail: gm92@tx.technion.ac.il.

ORCID

Jeffrey D. Rimer: 0000-0002-2296-3428

Notes

The authors declare no competing financial interest.

■ ACKNOWLEDGMENTS

Financial support for this project was provided by the Binational Science Foundation (Grant 2018344). J.D.R acknowledges additional financial support from The Welch Foundation (Grant E-1794).

■ REFERENCES

(1) Teketel, S.; Skistad, W.; Benard, S.; Olsbye, U.; Lillerud, K. P.; Beato, P.; Svelle, S. Shape selectivity in the conversion of methanol to hydrocarbons: the catalytic performance of one-dimensional 10-ring zeolites: ZSM-22, ZSM-23, ZSM-48, and EU-1. *ACS Catal.* **2012**, *2*, 26−37.

(2) Trakarnroek, S.; Jongpatiwut, S.; Rirksomboon, T.; Osuwan, S.; Resasco, D. E. n-Octane aromatization over Pt/KL of varying morphology and channel lengths. *Appl. Catal., A* **2006**, *313*, 189−199.

(3) Schulte, B.; Tsotsalas, M.; Becker, M.; Studer, A.; De Cola, L. Dynamic microcrystal assembly by nitroxide exchange reactions. *Angew. Chem., Int. Ed.* **2010**, *49*, 6881−6884.

(4) Lülf, H.; Bertucci, A.; Septiadi, D.; Corradini, R.; De Cola, L. Multifunctional inorganic nanocontainers for DNA and drug delivery into living cells. *Chem. - Eur. J.* **2014**, *20*, 10900−10904.

(5) Lupulescu, A. I.; Rimer, J. D. *In situ* imaging of silicalite-1 surface growth reveals the mechanism of crystallization. *Science* **2014**, *344*, 729−732.

(6) Rimer, J. D.; Trofymluk, O.; Navrotsky, A.; Lobo, R. F.; Vlachos, D. G. Kinetic and thermodynamic studies of silica nanoparticle dissolution. *Chem. Mater.* **2007**, *19*, 4189−4197.

(7) Kumar, M.; Li, R.; Rimer, J. D. Assembly and evolution of amorphous precursors in zeolite L crystallization. *Chem. Mater.* **2016**, *28*, 1714−1727.

(8) Farmanesh, S.; Ramamoorthy, S.; Chung, J.; Asplin, J. R.; Karande, P.; Rimer, J. D. Specificity of growth inhibitors and their cooperative effects in calcium oxalate monohydrate crystallization. *J. Am. Chem. Soc.* **2014**, *136*, 367−376.

(9) Chung, J.; Granja, I.; Taylor, M. G.; Mpourmpakis, G.; Asplin, J. R.; Rimer, J. D. Molecular modifiers reveal a mechanism of pathological crystal growth inhibition. *Nature* **2016**, *536*, 446−450.

(10) Olafson, K. N.; Ketchum, M. A.; Rimer, J. D.; Vekilov, P. G. Mechanisms of hematin crystallization and inhibition by the antimalarial drug chloroquine. *Proc. Natl. Acad. Sci. U. S. A.* **2015**, *112*, 4946−4951.

(11) Stephenson, A. E.; DeYoreo, J. J.; Wu, L.; Wu, K. J.; Hoyer, J.; Dove, P. M. Peptides enhance magnesium signature in calcite: insights into origins of vital effects. *Science* **2008**, *322*, 724−727.

(12) Lupulescu, A. I.; Rimer, J. D. Tailoring silicalite-1 crystal morphology with molecular modifiers. *Angew. Chem., Int. Ed.* **2012**, *51*, 3345−3349.

(13) Aizenberg, J.; Weaver, J. C.; Thanawala, M. S.; Sundar, V. C.; Morse, D. E.; Fratzl, P. Skeleton of Euplectella sp.: structural hierarchy from the nanoscale to the macroscale. *Science* **2005**, *309*, 275−278.

(14) Peng, X.; Manna, L.; Yang, W.; Wickham, J.; Scher, E.; Kadavanich, A.; Alivisatos, A. P. Shape control of CdSe nanocrystals. *Nature* **2000**, *404*, 59−61.

(15) Huang, W.-C.; Lyu, L.-M.; Yang, Y.-C.; Huang, M. H. Synthesis of Cu_2O nanocrystals from cubic to rhombic dodecahedral structures and their comparative photocatalytic activity. *J. Am. Chem. Soc.* **2012**, *134*, 1261−1267.

(16) Olafson, K. N.; Nguyen, T. Q.; Rimer, J. D.; Vekilov, P. G. Antimalarials inhibit hematin crystallization by unique drug−surface site interactions. *Proc. Natl. Acad. Sci. U. S. A.* **2017**, *114*, 7531−7536.

(17) Jones, F.; Richmond, W. R.; Rohl, A. L. Molecular modeling of phosphonate molecules onto barium sulfate terraced surfaces. *J. Phys. Chem. B* **2006**, *110*, 7414−7424.

(18) Farmanesh, S.; Alamani, B. G.; Rimer, J. D. Identifying alkali metal inhibitors of crystal growth: a selection criterion based on ion pair hydration energy. *Chem. Commun.* **2015**, *51*, 13964−13967.

(19) Lupulescu, A. I.; Kumar, M.; Rimer, J. D. A facile strategy To design zeolite L crystals with tunable morphology and surface architecture. *J. Am. Chem. Soc.* **2013**, *135*, 6608−6617.

(20) Doxey, A. C.; Yaish, M. W.; Griffith, M.; McConkey, B. J. Ordered surface carbons distinguish antifreeze proteins and their ice-binding regions. *Nat. Biotechnol.* **2006**, *24*, 852−855.

(21) Chen, C.-L.; Qi, J.; Tao, J.; Zuckermann, R. N.; DeYoreo, J. J. Tuning calcite morphology and growth acceleration by a rational design of highly stable protein-mimetics. *Sci. Rep.* **2015**, *4*, 6266.

(22) Elhadj, S.; De Yoreo, J. J.; Hoyer, J. R.; Dove, P. M. Role of molecular charge and hydrophilicity in regulating the kinetics of crystal growth. *Proc. Natl. Acad. Sci. U. S. A.* **2006**, *103*, 19237−19242.

(23) De Yoreo, J. J.; Vekilov, P. G. Principles of crystal nucleation and growth. *Rev. Mineral. Geochem.* **2003**, *54*, 57−93.

DOI: 10.1021/acs.chemmater.7b03798
Chem. Mater. 2017, 29, 9536−9546

(24) Lutsko, J. F.; González-Segredo, N.; Durán-Olivencia, M. A.; Maes, D.; Van Driessche, A. E. S.; Sleutel, M. Crystal growth cessation revisited: the physical basis of step pinning. *Cryst. Growth Des.* **2014**, *14*, 6129−6134.
(25) De Yoreo, J. J.; Gilbert, P. U. P. A.; Sommerdijk, N. A. J. M.; Penn, R. L.; Whitelam, S.; Joester, D.; Zhang, H.; Rimer, J. D.; Navrotsky, A.; Banfield, J. F.; Wallace, A. F.; Michel, F. M.; Meldrum, F. C.; Cölfen, H.; Dove, P. M. Crystallization by particle attachment in synthetic, biogenic, and geologic environments. *Science* **2015**, *349*, aaa6760.
(26) Lupulescu, A. I.; Qin, W.; Rimer, J. D. Tuning zeolite precursor interactions by switching the valence of polyamine modifiers. *Langmuir* **2016**, *32*, 11888−11898.
(27) Kumar, M.; Luo, H.; Román-Leshkov, Y.; Rimer, J. D. SSZ-13 crystallization by particle attachment and deterministic pathways to crystal size control. *J. Am. Chem. Soc.* **2015**, *137*, 13007−13017.
(28) Jo, C.; Jung, J.; Shin, H. S.; Kim, J.; Ryoo, R. Capping with multivalent surfactants for zeolite nanocrystal synthesis. *Angew. Chem., Int. Ed.* **2013**, *52*, 10014−10017.
(29) Xu, D.; Feng, J.; Che, S. An insight into the role of the surfactant CTAB in the formation of microporous molecular sieves. *Dalton Trans.* **2014**, *43*, 3612−3617.
(30) Qi, L.; Cölfen, H.; Antonietti, M. Control of Barite morphology by double-hydrophilic block copolymers. *Chem. Mater.* **2000**, *12*, 2392−2403.
(31) Yu, S.-H.; Colfen, H.; Tauer, K.; Antonietti, M. Tectonic arrangement of $BaCO_3$ nanocrystals into helices induced by a racemic block copolymer. *Nat. Mater.* **2005**, *4*, 51−55.
(32) Cai, A. J.; Guo, A. Y.; Chang, Y. F.; Sun, Y. F.; Xing, S. T.; Ma, Z. C. Fast synthesis of DNA-assisted flower-like ZnO superstructures with improved photocatalytic and antibacterial performances. *Mater. Lett.* **2013**, *111*, 158−160.
(33) Sonnichsen, F.; Sykes, B.; Chao, H.; Davies, P. The nonhelical structure of antifreeze protein type III. *Science* **1993**, *259*, 1154−1157.
(34) Liou, Y.-C.; Tocilj, A.; Davies, P. L.; Jia, Z. Mimicry of ice structure by surface hydroxyls and water of a β-helix antifreeze protein. *Nature* **2000**, *406*, 322−324.
(35) Farmanesh, S.; Chung, J.; Sosa, R. D.; Kwak, J. H.; Karande, P.; Rimer, J. D. Natural promoters of calcium oxalate monohydrate crystallization. *J. Am. Chem. Soc.* **2014**, *136*, 12648−12657.
(36) Friddle, R. W.; Weaver, M. L.; Qiu, S. R.; Wierzbicki, A.; Casey, W. H.; De Yoreo, J. J. Subnanometer atomic force microscopy of peptide−mineral interactions links clustering and competition to acceleration and catastrophe. *Proc. Natl. Acad. Sci. U. S. A.* **2010**, *107*, 11−15.
(37) Zhao, X.; Nagai, Y.; Reeves, P. J.; Kiley, P.; Khorana, H. G.; Zhang, S. Designer short peptide surfactants stabilize G protein-coupled receptor bovine rhodopsin. *Proc. Natl. Acad. Sci. U. S. A.* **2006**, *103*, 17707−17712.
(38) Zuckermann, R. N.; Kerr, J. M.; Kent, S. B. H.; Moos, W. H. Efficient method for the preparation of peptoids [oligo(N-substituted glycines)] by submonomer solid-phase synthesis. *J. Am. Chem. Soc.* **1992**, *114*, 10646−10647.
(39) Jiao, F.; Chen, Y.; Jin, H.; He, P.; Chen, C.-L.; De Yoreo, J. J. Self-repair and patterning of 2D membrane-like peptoid materials. *Adv. Funct. Mater.* **2016**, *26*, 8960−8967.
(40) Kudirka, R.; Tran, H.; Sanii, B.; Nam, K. T.; Choi, P. H.; Venkateswaran, N.; Chen, R.; Whitelam, S.; Zuckermann, R. N. Folding of a single-chain, information-rich polypeptoid sequence into a highly ordered nanosheet. *Biopolymers* **2011**, *96*, 586−595.
(41) Kirshenbaum, K.; Barron, A. E.; Goldsmith, R. A.; Armand, P.; Bradley, E. K.; Truong, K. T. V.; Dill, K. A.; Cohen, F. E.; Zuckermann, R. N. Sequence-specific polypeptoids: a diverse family of heteropolymers with stable secondary structure. *Proc. Natl. Acad. Sci. U. S. A.* **1998**, *95*, 4303−4308.
(42) Sanborn, T. J.; Wu, C. W.; Zuckermann, R. N.; Barron, A. E. Extreme stability of helices formed by water-soluble poly-N-substituted glycines (polypeptoids) with α-chiral side chains. *Biopolymers* **2002**, *63*, 12−20.
(43) Miller, S. M.; Simon, R. J.; Ng, S.; Zuckermann, R. N.; Kerr, J. M.; Moos, W. H. Comparison of the proteolytic susceptibilities of homologous L-amino-acid, D-amino-acid, and N-substituted glycine peptide and peptoid oligomers. *Drug Dev. Res.* **1995**, *35*, 20−32.
(44) Olivier, G. K.; Cho, A.; Sanii, B.; Connolly, M. D.; Tran, H.; Zuckermann, R. N. Antibody-mimetic peptoid nanosheets for molecular recognition. *ACS Nano* **2013**, *7*, 9276−9286.
(45) Bradley, E. K.; Kerr, J. M.; Richter, L. S.; Figliozzi, G. M.; Goff, D. A.; Zuckermann, R. N.; Spellmeyer, D. C.; Blaney, J. M. NMR structural characterization of oligo-N-substituted glycine lead compounds from a combinatorial library. *Mol. Diversity* **1997**, *3*, 1−15.
(46) Nam, K. T.; Shelby, S. A.; Choi, P. H.; Marciel, A. B.; Chen, R.; Tan, L.; Chu, T. K.; Mesch, R. A.; Lee, B.-C.; Connolly, M. D.; Kisielowski, C.; Zuckermann, R. N. Free-floating ultrathin two-dimensional crystals from sequence-specific peptoid polymers. *Nat. Mater.* **2010**, *9*, 454−460.
(47) Zuckermann, R. N.; Martin, E. J.; Spellmeyer, D. C.; Stauber, G. B.; Shoemaker, K. R.; Kerr, J. M.; Figliozzi, G. M.; Goff, D. A.; Siani, M. A.; Simon, R. J.; Banville, S. C.; Brown, E. G.; Wang, L.; Richter, L. S.; Moos, W. H. Discovery of nanomolar ligands for 7-transmembrane G-protein-coupled receptors from a diverse N-(substituted)glycine peptoid library. *J. Med. Chem.* **1994**, *37*, 2678−2685.
(48) Rosales, A. M.; Segalman, R. A.; Zuckermann, R. N. Polypeptoids: a model system to study the effect of monomer sequence on polymer properties and self-assembly. *Soft Matter* **2013**, *9*, 8400−8414.
(49) Shin, S. B. Y.; Kirshenbaum, K. Conformational rearrangements by water-soluble peptoid foldamers. *Org. Lett.* **2007**, *9*, 5003−5006.
(50) Baskin, M.; Maayan, G. A rationally designed metal-binding helical peptoid for selective recognition processes. *Chem. Sci.* **2016**, *7*, 2809−2820.
(51) Gangloff, N.; Ulbricht, J.; Lorson, T.; Schlaad, H.; Luxenhofer, R. Peptoids and polypeptoids at the frontier of supra- and macromolecular engineering. *Chem. Rev.* **2016**, *116*, 1753−1802.
(52) Chen, C.-L.; Qi, J.; Zuckermann, R. N.; DeYoreo, J. J. Engineered biomimetic polymers as tunable agents for controlling $CaCO_3$ mineralization. *J. Am. Chem. Soc.* **2011**, *133*, 5214−5217.
(53) Maayan, G.; Liu, L.-K. Silver nanoparticles assemblies mediated by functionalized biomimetic oligomers. *Biopolymers* **2011**, *96*, 679−687.
(54) Robinson, D. B.; Buffleben, G. M.; Langham, M. E.; Zuckermann, R. N. Stabilization of nanoparticles under biological assembly conditions using peptoids. *Biopolymers* **2011**, *96*, 669−678.
(55) Tigger-Zaborov, H.; Maayan, G. Nanoparticles assemblies on demand: Controlled aggregation of Ag(0) mediated by modified peptoid sequences. *J. Colloid Interface Sci.* **2017**, *508*, 56−64.
(56) Huang, M. L.; Ehre, D.; Jiang, Q.; Hu, C.; Kirshenbaum, K.; Ward, M. D. Biomimetic peptoid oligomers as dual-action antifreeze agents. *Proc. Natl. Acad. Sci. U. S. A.* **2012**, *109*, 19922−19927.
(57) Reyes, F. T.; Guo, L.; Hedgepeth, J. W.; Zhang, D.; Kelland, M. A. First investigation of the kinetic hydrate inhibitor performance of poly(N-alkylglycine)s. *Energy Fuels* **2014**, *28*, 6889−6896.
(58) Tamm, P. W.; Mohr, D. H.; Wilson, C. R. Octane enhancement by selective reforming of light paraffins. *Stud. Surf. Sci. Catal.* **1988**, *38*, 335−353.
(59) Larlus, O.; Valtchev, V. P. Crystal morphology control of LTL-type zeolite crystals. *Chem. Mater.* **2004**, *16*, 3381−3389.
(60) Itani, L.; Bozhilov, K. N.; Clet, G.; Delmotte, L.; Valtchev, V. Factors that control zeolite L crystal size. *Chem. - Eur. J.* **2011**, *17*, 2199−2210.
(61) Lee, Y.-J.; Lee, J. S.; Yoon, K. B. Synthesis of long zeolite-L crystals with flat facets. *Microporous Mesoporous Mater.* **2005**, *80*, 237−246.
(62) Megelski, S.; Calzaferri, G. Tuning the size and shape of zeolite L-based inorganic−organic host−guest composites for optical antenna systems. *Adv. Funct. Mater.* **2001**, *11*, 277−286.
(63) Crapster, J. A.; Guzei, I. A.; Blackwell, H. E. A peptoid ribbon secondary structure. *Angew. Chem., Int. Ed.* **2013**, *52*, 5079−5084.

DOI: 10.1021/acs.chemmater.7b03798
Chem. Mater. 2017, 29, 9536−9546

(64) Caumes, C.; Hjelmgaard, T.; Remuson, R.; Faure, S.; Taillefumier, C. Highly convenient gram-scale solution-phase peptoid synthesis and orthogonal side-chain post-modification. *Synthesis* **2011**, *2011*, 257−264.
(65) Gaona-Gómez, A.; Cheng, C.-H. Modification of zeolite L (LTL) morphology using diols, $(OH)_2(CH_2)_{2n+2}O_n$ (n = 0, 1, and 2). *Microporous Mesoporous Mater.* **2012**, *153*, 227−235.
(66) Maldonado, M.; Oleksiak, M. D.; Chinta, S.; Rimer, J. D. Controlling crystal polymorphism in organic-free synthesis of Na-zeolites. *J. Am. Chem. Soc.* **2013**, *135*, 2641−2652.
(67) Conato, M. T.; Oleksiak, M. D.; Peter McGrail, B.; Motkuri, R. K.; Rimer, J. D. Framework stabilization of Si-rich LTA zeolite prepared in organic-free media. *Chem. Commun.* **2015**, *51*, 269−272.
(68) Townsend, E. R.; van Enckevort, W. J. P.; Meijer, J. A. M.; Vlieg, E. Polymer versus monomer action on the growth and habit modification of sodium chloride crystals. *Cryst. Growth Des.* **2015**, *15*, 5375−5381.
(69) Mannhold, R.; Rekker, R. F. The hydrophobic fragmental constant approach forcalculating log P in octanol/water and aliphatic hydrocarbon/water systems. *Perspect. Drug Discovery Des.* **2000**, *18*, 1−18.
(70) Haynes, W. M., Ed. *CRC handbook of chemistry and physics*, 97th ed.; CRC Press: Boca Raton, FL, USA, 2016.
(71) Hine, J.; Hine, M. The relative acidity of water, methanol and other weak acids in isopropyl alcohol solution 1. *J. Am. Chem. Soc.* **1952**, *74*, 5266−5271.
(72) Perrin, D. The effect of temperature on pK values of organic bases. *Aust. J. Chem.* **1964**, *17*, 484−488.
(73) Oleksiak, M. D.; Soltis, J. A.; Conato, M. T.; Penn, R. L.; Rimer, J. D. Nucleation of FAU and LTA zeolites from heterogeneous aluminosilicate precursors. *Chem. Mater.* **2016**, *28*, 4906−4916.
(74) Greer, H.; Wheatley, P. S.; Ashbrook, S. E.; Morris, R. E.; Zhou, W. Early stage reversed crystal growth of zeolite A and its phase transformation to sodalite. *J. Am. Chem. Soc.* **2009**, *131*, 17986−17992.
(75) Mintova, S.; Olson, N. H.; Bein, T. Electron microscopy reveals the nucleation mechanism of zeolite Y from precursor colloids. *Angew. Chem., Int. Ed.* **1999**, *38*, 3201−3204.

DOI: 10.1021/acs.chemmater.7b03798
Chem. Mater. 2017, 29, 9536−9546